Received: 9 September 2020 | Revised: 6 November 2020 | Accepted: 20 November 2020

DOI: 10.1002/er.6267

SPECIAL ISSUE REVIEW PAPER

INTERNATIONAL JOURNAL OF ENERGY RESEARCH WILEY

Processing of fast neutron reactor fuel by electrorefining: Thematic overview

Alexander Y. Galashev[1,2]

[1]Institute of High-Temperature Electrochemistry, Ural Branch, Russian Academy of Sciences, Yekaterinburg, Russia

[2]Institute of Chemical Technology, Ural Federal University named after the First President of Russia B.N. Yeltsin, Yekaterinburg, Russia

Correspondence
Alexander Y. Galashev, Institute of High-Temperature Electrochemistry, Ural Branch, Russian Academy of Sciences, Academic Str. 20, Yekaterinburg 620990, Russia.
Email: galashev@ihte.uran.ru

Funding information
State Atomic Energy Corporation ROSATOM, Grant/Award Number: H.4o.241.19.20.1048 dated Apr

Summary

This work provides basic knowledge on the spent fuel management on the basis of the published literature data on electrorefining. This review examines three main areas of work devoted to electrorefining. These are electrodeposition and electrodissolution using solid and liquid electrodes, as well as mass transfer in phases present during electrorefining. As part of this research, the composition of the irradiated metallic fuel was estimated. Due to the great potential difference between solid cathodes, it is possible to separate actinides from lanthanides. The co-deposition of metallic Pu and U in the eutectic LiCl-KCl melt containing UCl_3 and $PuCl_3$ indicates stable co-precipitation of U and Pu at U^{3+} concentration less than ~0.2 wt. Periodically performed electrical transport of ions to liquid (Cd) and solid cathodes in the galvanic mode made it possible to deposit preferentially U on the solid cathode, and Pu and Am on the liquid cathode. Oxidation of these metals caused fluctuations in the anode potential. The electrode processing after electrorefining is investigated. This process consists of oxidizing the actinides remaining in the liquid electrode by adding $CdCl_2$ and removing the associated chloride by high-temperature distillation. During the electrorefining of irradiated metallic fuel, the fission products accumulate in the molten salt. Reduction of uranium on a solid cathode from a spent molten salt using a liquid Cd-Li anode is considered. A model that describes electrorefining with a liquid metal anode, solid cathode, and molten LiCl-KCl salts, is presented. The formation of plutonium at the surface of a solid cathode is analyzed. In a one-dimensional model of an electrorefiner, it is shown that the concentration of Pu at the cathode cannot be predicted from the Cm concentration in the melt.

KEYWORDS

electrolyzer, experiment, model, plutonium, spent nuclear fuel, uranium

1 | INTRODUCTION

To date, there are different opinions about the development of the nuclear power industry. On the one hand, nuclear power plants, due to their high inertia, ensure grid stability and do not pollute the environment with CO_2 emissions. On the other hand, there is a risk of radioactive contamination of the area and the problems of storage and processing of radioactive waste remain unresolved. Regardless of the decision to continue or to stop the production of nuclear energy, the solution to the problem of spent nuclear fuel (SNF) management

remains urgent.[1] This is primarily due to the fact that SNF radioactivity preserves for a long time and the problem of radiation safety will remain relevant for future generations.

Nuclear power will become the most attractive among any other energy generating industries if the problem of nuclear waste is solved. In future, most of the spent fuel will be reprocessed, but today, the main direction of reprocessing is the extraction of plutonium and uranium. Selective dissolution and deposition of metals can be carried out in molten chlorides, such as molten alkali metal salts. A wide range of salt melts, including their mixtures, provides solvents with the required electrochemical properties and high radiation resistance.[2] The SNF is mainly processed by electrorefining, where LiCl-KCl melt is used as a solvent at an operating temperature of about 500°C. Unlike aqueous solutions and organic media, metal salts are not neutron moderators.

An electrorefining method allows the removal of impurities from metal, which cannot be removed by any economical alternative processes. The current density is one of the most important parameters of the electrorefining process. It is determined by the applied electrode potential. The current density has a great influence on the dissolution of metals at the anode, and at the cathode, it largely determines the co-precipitation of impurities. Increased current densities create conditions for increase in production capacity but are reflected in the purity and morphology of cathodic deposition. In reality, electrorefining is a process that can be performed with different levels of complexity. The quantity and quality of the final product obtained in this process are influenced by many factors. Control over this process is in many ways complicated by the interdependence of the parameters that determine the passage of the process.

The method for recovering and recycling of metallic fuel from a fast reactor was originally developed by Argonne National Laboratory (ANL). Until now, this method, which implies using a liquid cadmium electrode, has no alternative. The liquid cadmium pool functions as an intermediate electrode during the SNF electrorefining process. With the participation of a liquid cadmium electrode, actinides separate from the fission products. The spent fuel electrorefining is usually carried out in a molten LiC1-KCl/liquid cadmium system. In addition, the use of liquid cadmium in the electrorefining process makes it possible to develop more compact processes for the separation of actinides and to reduce the amount of radioactive waste. Uranium, plutonium, and other actinides, which are oxidized at the anode enter the cadmium bath, where they are reduced with liquid cadmium.

Almost three decades have passed since the publication of one of the most complete reviews[3] on the electrorefining via the pyrochemical reduction of fuel from fast reactors. Since then, many important works have been carried out to improve the efficiency of spent metallic fuel (SMF) processing. In this literature review, we analyze new experimental and theoretical research that could dramatically improve the SMF processing. The review is structured to reflect three main areas of the electrorefining process: (a) anodic dissolution, also called oxidation or electrodissolution, (b) mass transfer (in molten salt), and (c) cathodic deposition or electrodeposition at solid and liquid cathodes. All three operations considered by us are interrelated and the assignment of any of the works to one of these directions is not strict. Nevertheless, we tried to be more objective and made a selection based on the most significant, in our opinion, result obtained in this study.

The technological progress provided regulation of nuclear power based on load and even made it compatible with renewable power sources.[4] Low prices for uranium and the absence of shortage in this type of fuel, as well as some technical problems, slowed down the development of technology for SNF reprocessing. However, recently, the concept of spent reactor fuel reprocessing and especially the plutonium extraction has become increasingly relevant. This is due to the accumulation of a huge amount of SNF and the problems associated with its storage. Creation of an efficient technology for SNF reprocessing will close the nuclear fuel cycle and will largely solve the problem of SNF disposal.

Electrorefining can become the final stage of pyroprocessing, which aims at processing of spent oxide fuel from light water reactors for fast reactors. Such reprocessing of SNF will increase the efficiency of uranium use and will reduce the amount of hazardous radioactive waste. Electrorefining purifies uranium and plutonium-containing actinides.

This review focuses on the electrorefining process and has the following form. Before the analysis of the process itself, we present some basic provisions, which clarify the description of the electrorefining process. We will consider in detail what constitutes the starting material for electrorefining, that is, SNF. We also pay attention to the theoretical approach to the description of the electrolysis process and, finally, we will consider a schematic diagram of the SNF electrorefining process.

The electrorefining process analysis includes the following stages. First, the cathode deposition on a solid electrode, which allows evaluating the quality of the final product, is considered. The cathode deposition is substantially wider analyzed in the literature. Therefore, we will consider the electrodeposition on liquid and solid

cathodes separately. In our opinion, the topic of deposition of heavy metals on a liquid cathode is of greatest interest. That is why, we will consider it first, and then briefly highlight the works associated with cathode deposition on a solid electrode. After that, the phenomenon of mass transfer in the melt will be considered, and finally, the oxidation process, that is, the dissolution of the material loaded into the anode basket will be analyzed. This sequence of presentation allows us to consider the process of electrorefining from a more natural and practical point of view.

The purpose of this work is to present in an accessible form some of the most important studies, where the electrorefining method is used as one of the stages of processing of SNF extracted from thermal and fast reactors.

2 | SPENT NUCLEAR FUEL

The fission process in a nuclear reactor changes the physical state of the fuel. At the same time, its chemical composition is also transformed, since fission products are new elements. In addition, a change in the chemical composition occurs not only due to the nuclear fission, but also due to the absorption of neutrons by uranium nuclei and their subsequent decay. As a result, transuranic elements such as neptunium, plutonium, americium, and curium are formed. These elements are also involved in the nuclear fuel cycle. In a nuclear reactor, inelastic collisions with other atoms result in the loss of energy of energy fission fragments on their way through the fuel. Atoms knocked out of their places of residence by direct collisions interact with other atoms, creating collisions and displacement cascades in the material. These processes cause the heat generation in the reactor, which is removed from the reactor and is subsequently used to generate electricity or for other purposes.

In an operating nuclear reactor, part of the fuel is periodically replaced. Initially, a discharged fuel has a very high level of radioactivity. The composition of the fuel changes due to burnout. Thus, in thermal reactors, the fresh fuel has an approximate composition of 3% ^{235}U and 97% ^{238}U (in terms of U). At the same time, the amount of uranium in the seized fuel is decreasing (approximately 1% ^{235}U and 94% ^{238}U). However, SNF contains Pu isotopes and fission products. Unlike long-lived emitters, the β emitters do not contribute much to heat generation due to their shorter half-lives.

The conversion of an oxide fuel such as UO_2 to metal is carried out using electrolytic reduction, roughly described by a generalized reaction:

$$UO_2(s) + 4\,Li(l) \rightarrow U(s) + 2\,Li_2O. \quad (1)$$

The theoretical understanding of this process and its modeling are provided in the works.[5-8] In fact, the final product obtained as a result of electrolytic reduction, in addition to U, can contain Pu and minor actinides (MA), noble metals, and decay products. A product of this complex composition can then be processed by electrorefining. The separation process of electrorefining is important in the processing of some SNF, recovered heavy metal, especially metal jet fuel. The uniqueness of such fuel lies in the fact that it cannot be adapted to geologic disposal in its intrinsic form. Electrorefining is the electroextraction of pure metal from a corresponding metal containing impurities, or from an alloy that is placed in a solution or molten salt.

The metallic fuel is intended for fast reactors. Fast reactors do not need neutron moderators (water or graphite). Such reactors have a 'hard' neutron energy spectrum compared to 'thermal reactors'. The metallic fuel is an injection casting of the binary (U-Pu), (U-Zr), or ternary (U-Pu-Zr) alloys.[9,10] The thermal conductivity of a metallic fuel is an order of magnitude higher than that of an oxide fuel. In addition, metallic fuel has a lower heat capacity. Consequently, for this type of fuel, peak temperatures are reduced and it is easier to cool it. The use of such fuel allows one to burn actinides and to obtain additional fuel and to reduce the waste stream. The composition of the fuel elements of a fast reactor changes due to the irradiation and isotope fission. These changes are approximately reflected in Figure 1. A radioactive decay is accompanied by the release of alpha and beta particles from nuclei, as well as the emission of gamma rays. As a result of these processes, the fuel assemblies are heated. The heat generated is used for consumer needs, mainly for power generation.

Zirconium alloy is used both in light water reactors (for cladding nuclear fuel) and in fast reactors (as a fuel component). Zr combines good corrosion resistance in the water chemistry at 300°C and low capture cross-section for thermal neutrons.

High-temperature reprocessing of SMF is defined as a nonaqueous process of a number of chemical separations undertaken to purify and recover actinides from SMF. Metallic fuel consists mainly of U-Zr or U-Pu-Zr alloys. Electrorefining uses the difference in the transport of uranium, plutonium, and fission products in molten metals and salts. The presence of zirconium in it provides a sufficiently high melting point of the fuel.[11] Zirconium also prevents swelling of metallic fuels due to irradiation. The redox potential of zirconium is close to the potential of uranium. That is why the part of the zirconium dissolves

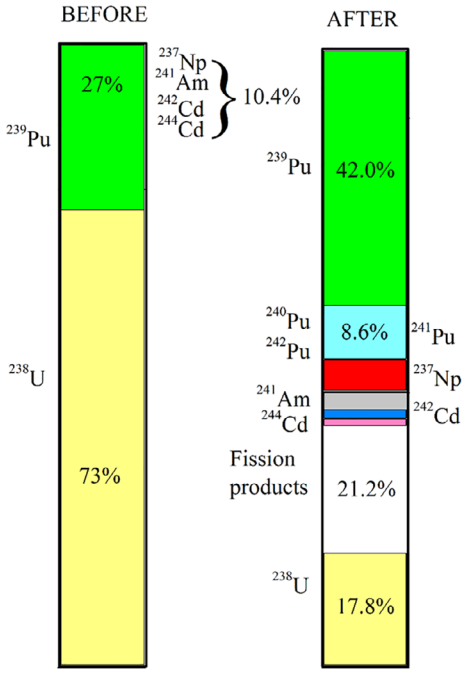

FIGURE 1 Changes in the chemical composition of the irradiated metallic U-Pu fuel [Colour figure can be viewed at wileyonlinelibrary.com]

when the refining process is carried out until a very low residual presence of actinides is achieved, or a higher dissolution rate is created by a high density of the anode current.

A study of pyrochemical reprocessing of SNF in the LiC1-KC1 eutectic mixture at 773 K and a study of electric transport from the cadmium cathode was performed in Reference 12. However, the data needed for designing and evaluating the effectiveness of the electrorefining process still required further specification.

3 | THEORETICAL DESCRIPTION OF ELECTROLYSIS

During refining, a suitable electrical potential is applied between these electrodes, which makes it possible for the atoms present in the anode to oxidize and the electrolyte atoms to be reduced. The correct selection of the interelectrode potential enables a selective transfer of pure metal from the anode to the cathode. The selection of the potential initiating this process can be made according to the Nernst equation:

$$E_a = E^0 + \frac{RT}{zF}\ln Q_r, \tag{2}$$

where E_a is the cell voltage, E^0 is the standard cell potential, R is the ideal gas constant (8.314 J K^{-1} mol^{-1}), T is the absolute temperature (K), F = 96 485 C mol^{-1} is the Faraday constant, and Q_r the reaction quotient,[13] which is defined as:

$$Q_r = \frac{a_i^m \cdot a_j^n}{a_k^p \cdot a_l^q} = \frac{\Pi(\text{products})}{\Pi(\text{reactants})}, \tag{3}$$

where Π represents the product of the concentrations (activities, a) raised to the power of their stoichiometric numbers.

Using the first Faraday's law, one can determine the mass of the substance released at the anode:

$$m = \left(\frac{Q}{F}\right)\cdot\left(\frac{M}{z}\right), \tag{4}$$

where Q is the total electric charge passed between electrodes, M is the molar mass of the metal, z is the valency number of ions of the metal, and m is the mass of the metal liberated.[14]

The electrolysis process is interfered by the chemical irreversibility, which is responsible for the resulting overvoltage. Overvoltage is defined as the difference between the thermodynamically expected reduction potential and the potential at which the reduction actually occurs. The actual energy required to start the reaction is almost always higher than the energy determined by thermodynamic calculation. The external manifestation of this difference is the heat generation. The overpotential is influenced by the cell design and operating conditions.[14] The current efficiency (CE) characterizes the sum of all losses in the electrolytic cell and is defined as the ratio of the mass actually released at the cathode to the theoretical mass calculated using integral characteristics.

To carry out the electrorefining process, an unclean metallic anode and a cathode are placed in an electrolyte solution. An electrical potential is applied between these electrodes, which causes oxidation of the impure metal, that is, metal atoms lose their electrons. As a result, the neutral metal atoms that constitute the anode turn into ions. There are three ways to deliver ions to the electrode: diffusion, convection, and migration. Diffusion occurs due to the presence of a concentration gradient. Molecules migrate under the influence of an electric gradient. Bulk movement of the medium or convection occurs due to the organized collective movement of molecules. In the presence of these three movements in the area adjacent to the electrode, a reduced concentration of ions is

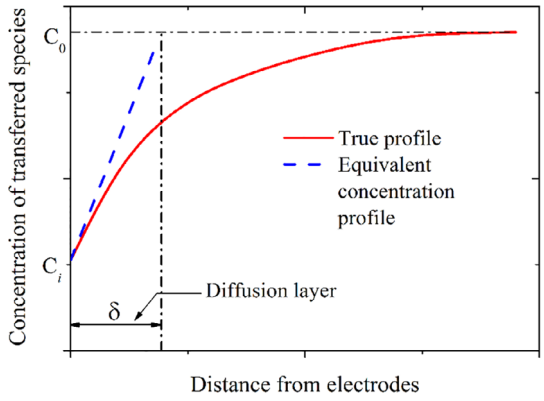

FIGURE 2 Concentration gradient vs distance from the electrode. The concentration of ions decreases greatly in the direct vicinity of the electrode [Colour figure can be viewed at wileyonlinelibrary.com]

created. This situation is reflected in Figure 2. The higher electric current density results in the faster the outflow of ions surrounding the electrode, and hence, the concentration gradient increases. Finally, the concentration of ions on the electrode may reach zero value. The current corresponding to this process is called limiting. In this case, the reaction rate is controlled by the rate of mass transfer to the electrode. A further increase in the current (above the limit value) leads to an increase in the electrode potential. Finally, the potential reaches a value when a new reaction is triggered. Diffusion is the main process in electrorefining. If migration and convection contribute slightly to the motion of ions, then at zero concentration of ions on the electrode, we have an expression for the limiting current:

$$i_L = \frac{zFDC}{\delta}, \tag{5}$$

where z is the valence of an ion, D is the ion diffusion coefficient in the melt, C is the concentration of ions, and δ is the thickness of the diffusion layer.

The controlled reaction rate can be increased by increasing the mass transfer to the electrode. The reaction rate is influenced by the current density and stirring. The mass transfer can be increased by limiting the current to such a value, at which the concentration gradient is maximized. Moreover, of the melt, stirring increases the convection through the boundary layer.

4 | ELECTROREFINING OF FUEL FROM A FAST NEUTRON REACTOR

The electrorefining process is carried out in a special cell in which the molten salt mixture (LiCl + KCl) is placed on liquid cadmium at the temperature of 773 K.[15] A schematic diagram of the electrorefining cell is shown in Figure 3. A steel basket loaded with SMF is used as an anode. The process of electrorefining includes the initial oxidation of all actinides that compose the SMF and their subsequent reduction in liquid cadmium. Uranium and a mixture of plutonium and uranium are transferred to a solid iron cathode and a liquid cadmium electrode, respectively. Oxidized alkali and alkaline earth metals remain in the molten salt. Nonoxidized precious metals such as ruthenium and palladium remain in the anode basket. An inert (Ar) atmosphere prevents oxygen oxidation at the surface of the molten salt.

The basic composition of SNF used during the electrorefining is U-Zr or U-Pu-Zr. Apart from that SNF contains MA. This complex SNF mixture is loaded into the anode basket (Figure 3). As a rule, the eutectic melt LiCl-KCl is used as an electrolyte. The anodic dissolution of the loaded SNF follows the reaction:

$$\mathrm{Xn} \rightarrow \mathrm{Xn}^{3+} + 3\mathrm{e}^{-}, (\mathrm{Xn}: \mathrm{U}; \mathrm{Pu}; \text{minor actinides(MA)}). \tag{6}$$

The function of a solid steel cathode is to collect U in the electrolyte bulk. This selective process is determined by the reaction:

$$\mathrm{U}^{3+} + 3\mathrm{e}^{-} \rightarrow \mathrm{U}. \tag{7}$$

The rest of U, as well as Pu and MA are reduced at the liquid cadmium cathode according to the reaction:

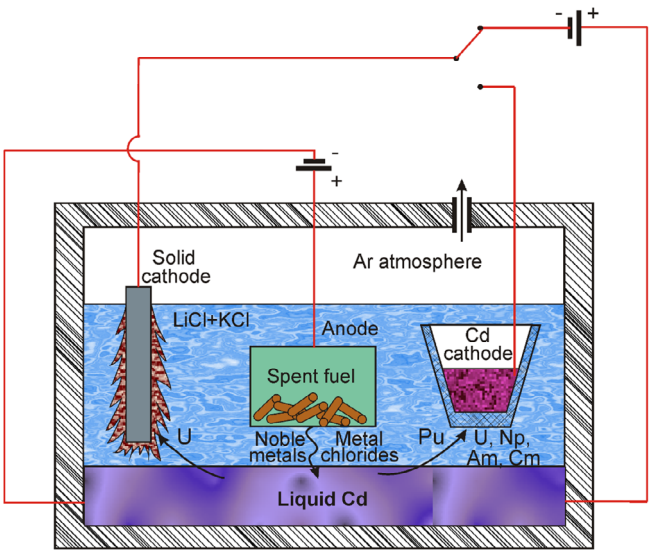

FIGURE 3 Schematic diagram of the electrorefining process[15] [Colour figure can be viewed at wileyonlinelibrary.com]

$$\left(U^{3+}, Pu^{3+}, \text{or } MA^{3+}\right) + 3e^- \rightarrow (U, Pu, \text{or MA}) \text{ in Cd}. \quad (8)$$

A portion of the rare earth elements is also reduced at the liquid Cd cathode. The remaining part of these elements together with alkaline and alkaline earth elements remains in the melt in the form of chlorides. To dissolve Zr, a more positive anode potential is required. Therefore, Zr, together with the fission products of the noble metals, remains in the anode basket.

5 | ELECTRODEPOSITION

Electrorefining of SNF is a complex process that separates the uranium from fission products. As a result of electrorefining, the amount of radioactive waste is reduced.[16,17] The liquid cadmium cathode plays a special role in the electrorefining process and can be considered as an intermediate electrode between the anode and the cathode. Almost pure uranium is transferred to a solid cathode.

5.1 | Molten salt electrorefining of U-Pu-Zr alloy fuel

Both SMF and reduced oxide fuel may be exposed to electrolysis-based pyrometallurgical processing. The recovery occurs both in the solid and liquid cathodes. Uranium is reduced on a solid electrode, and an alloy of uranium with trans-uranium elements is reduced on a liquid electrode. The electrorefining of the U-Pu alloy containing a small amount of Am was performed by Kuratal et al.[18] The separation factor among actinides determined by their content in liquid cadmium and salt was equal to 1.69 to 1.74 and 0.66 to 0.78 for U/Pu and Am/Pu, respectively. At the same time, the amount of Pu and Am in the anode residue decreased significantly compared to the original alloy composition.

Kuratal et al[18] used the U-Pu alloy containing a small amount of Am as a material loaded into the anode basket during the electrolysis. The actinide separation efficiency was evaluated using a separation factor (*SF*) determined from the actinide concentration in the Cd and salt samples:

$$SF = \frac{(\text{mole fraction of U or Am in Cd})/(\text{mole fraction of Pu in Cd})}{(\text{mole fraction of U or Am in salt})/(\text{mole fraction of Pu in salt})}. \quad (9)$$

The following essential conclusions were drawn in the aforesaid paper:

1. The anode dissolution rates of U, Pu, and Am from the U-Pu-Am alloy are different.
2. During the electrolysis, trivalent ions dissolve in a molten salt:

$$\text{Pu (or Am)} + UCl_3 = U + PuCl_3 \text{ (or } AmCl_3). \quad (10)$$

3. If an oxygen impurity is present in the U-Pu-Am alloy, the following chemical reaction appears:

$$U + (U, Pu, \text{or Am})O_x = UO \text{ (or } UO_2) + \text{Pu (or Am)}. \quad (11)$$

4. In the case of the sesquioxide of Pu and Am in the molten salt, the following two steps might proceed:

$$2UCl_3 + 3(\text{Pu or Am})_2O_3 = UO + UO_2 + 6(\text{Pu or Am})OCl, \quad (12)$$

and

$$2UCl_3 + 3(\text{Pu or Am})OCl = UO + UO_2 + 3(\text{Pu or Am})Cl_3. \quad (13)$$

These two equations describe the mass balance of Pu and Am and reflect the extraction of Pu and Am from various residues.

5. After the electrolysis, a small amount of $ZrCl_4$ reagent is added into the molten salt to convert the U metallic deposit to chloride. The changes occurring in the electrolyte and anode residue composition are reflected by the following equation:

$$4U + 3ZrCl_3 = 4UCl_3 + 3Zr. \quad (14)$$

In Reference 18, U-dendrites and U-Pu-Am alloys were simultaneously obtained at the iron cathode and in liquid cadmium, respectively.

Koyama et al[19] carried out the electrorefining of unirradiated U-20Pu-10Zr alloy. Metallic fuels are

anodically dissolved in a molten salt medium at around 773 K. The anode basket was not corroded after the electrorefining. The first refining step was carried out in the presence of a solid iron cathode, onto which a mixture of the deposited U (dendrites) and the chemically reduced U was transferred. The latter was formed as a result of the reaction between deposited Pu and UCl_3. Then, the next refining step was carried out using a liquid cadmium cathode. Chemical analysis showed that the CE based on the Cd ingot is only 77%. A solid deposit, formed on the crucible bottom, contained a relatively high Pu content of about 34 wt%. The reduction of Pu-U from Pu-U-Zr at the liquid Cd cathode was shown. However, the optimization of the conditions of this deposition remained unexplored.

Using the electrorefining process, the cladding of SNF can be reprocessed. Sohn et al[20] performed a simulation of the extraction of high-purity metallic Zr from the SNF shell (zircaloy-4). A numerical modeling based on the Butler-Volmer equation and hydrodynamics shows that a two-stage reduction of Zr (IV) to Zr with ZrCl is possible. Optimization of the design of the electrorefiner was carried out by considering the influence of the rotation of the electrodes and variation of the potentials and masses of molten salts, as well as numbers of anode baskets in the cell.

5.2 | Liquid cadmium cathode performance model

The present model is based on the equilibrium behavior of U and Pu in the molten LiCl-KCl/Cd system at 773 K.[21] When constructing the model, it was assumed that the following four phases were in a balance.

5.2.1 | Salt phase

The salt phase is always located above the liquidus surface, because it is assumed that no solid phases are released from the salt phase. The eutectic salt LiCl-KCl is the solvent in this system. The dissolved substances UCl_3 and $PuCl_3$ promote chemical exchange between different phases.

5.2.2 | Cd phase

Apart from pure Cd, this phase has inclusions in the form of Li, K, Pu, and U, and may also contain some $CdCl_2$. The phase behavior of the Cd-U-Pu alloy at 773 K limits the composition of this phase. The model illustrates the deposition of U and intermetallic $PuCd_6$ with the corresponding saturation of the phase with U or Pu elements.

5.2.3 | Metallic uranium phase

Uranium is present as UCl_3 and dissolved metallic U in the Salt phase and Cd phase, respectively. The intrinsic metallic U phase is formed when the cadmium is saturated with uranium.

5.2.4 | Intermetallic $PuCd_6$ phase

Plutonium may be present in the form of $PuCl_3$ or as dissolved metallic Pu in the salt phase and Cd phase, respectively. When plutonium saturation occurs in the Cd phase, an intermetallic compound $PuCd_6$, which deposits, forming its own phase, is formed.

The initial state of the system with to some extent arbitrary parameters is nonequilibrium. The model allows determining the equilibrium state of the system for each selected initial state by a set of parameters. Variables representing the initial conditions are independent only within certain limits. In particular, a situation, when concentrations of U and Pu are below their saturation limits and both metals are present as dissolved atoms in the Cd phase, is considered. In this case, UCl_3 and $PuCl_3$ are dissolved in a salt solvent, and the thermodynamic equilibrium between the Salt phase and the Cd phase is observed:

$$PuCl_3(\text{salt}) + U(\text{cadmium}) = UCl_3(\text{salt}) + Pu(\text{cadmium}). \quad (15)$$

The stoichiometry of this reaction, which proceeds in a liquid medium, gives an idea of the exchange of U and Pu between the two phases.

Two cases of the behavior of a liquid cadmium cathode (LCC) are of interest. The first case refers to an unsaturated state that crosses the Cd/U phase boundary in the diagram. When this phase boundary is reached, the LCC state appears to be supersaturated by U, and the release of metallic U phase begins. The unsaturated state, considered with respect to the $Cd/PuCd_6$ boundary, refers to the second case. This boundary is reached when a Pu supersaturation occurs and the intermetallic phase of $PuCd_6$ becomes visible. In the first case, the amount of salt in the model was 10 kg, and in the second case, it was 20 kg, while the amount of Cd in both cases was the same (1 kg).

We can define the separation coefficient (SF) as the Pu: U ratio in the salt phase divided by the Pu: U ratio in the cadmium phase:

$$SF_{true} = \frac{\frac{M_{PuCl_3}^{Salt\_phase}}{M_{UCl_3}^{Salt\_phase}}}{\frac{M_{Pu}^{Cd\_phase}}{M_{U}^{Cd\_phase}}}, \quad (16)$$

where $M_{PuCl_3}^{Salt\_phase}$ and $M_{UCl_3}^{Salt\_phase}$ are moles of $PuCl_3$ and UCl_3 in the salt phase, respectively; $M_{Pu}^{Cd\_phase}$ and $M_{U}^{Cd\_phase}$ are moles of Pu and U in the Cd phase, respectively.

A liquid cadmium phase contains dissolved U and Pu. In this case, the separation factor is defined as accurate or true. Figure 4 shows the change in this characteristic as U is loaded into the system. However, the situation changes somewhat, when the coexistence of the intermetallic phase of $PuCd_6$ and the metallic U phase is considered. Here, another interpretation is more suitable for SF, in which this characteristic is presented as the apparent SF:

$$SF_{Apparent} = \frac{\frac{M_{PuCl_3}^{Salt\_phase}}{M_{UCl_3}^{Salt\_phase}}}{\left(\frac{M_{Pu}^{Cd\_phase} + M_{Pu}^{PuCd_6\_phase}}{M_{U}^{Cd\_phase} + M_{U}^{U\_phase}}\right)}, \quad (17)$$

where $M_{Pu}^{PuCd_6\_phase}$ denoted the moles of Pu in the intermetallic phase of $PuCd_6$, $M_{U}^{U\_phase}$ denotes the moles of U in the metallic U phase.

It is clear that in the unsaturated state, the true SF and apparent SF are the same. However, this is not true in a supersaturated state, where true SF and apparent SF diverge significantly, as it is seen in Figure 5.

The simulation is mainly aimed at the evaluation of the performance of the liquid cadmium cathode with a gradual addition of U to the system. The SFs characterize in detail the steady performance of the thermodynamic model of the electrorefiner. The separation of total SF into true and apparent SF is made. The definition of true SF is based on the equilibrium between the salt phase and the cadmium phase. While the apparent SF is the result of a description of the procedure of Pu addition to the intermetallic phase of $PuCd_6$ and U addition to the metallic U phase. SF defined in this way has no thermodynamic meaning. The model is useful for estimation of the yield of intermediates in the electrorefining process.

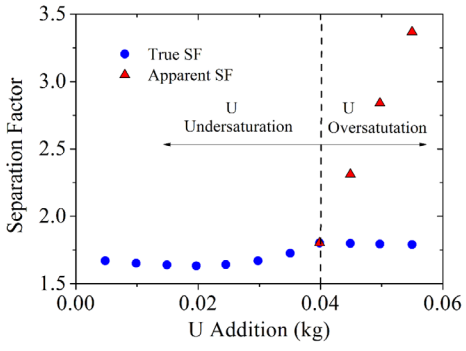

FIGURE 4 True and apparent separation factor (SF) depending on U addition for the first case under undersaturated and oversaturated conditions[21] [Colour figure can be viewed at wileyonlinelibrary.com]

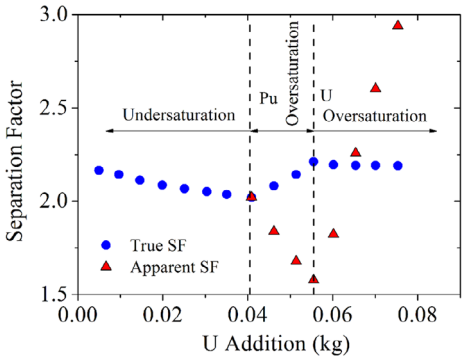

FIGURE 5 True and apparent separation factor (SF) depending on U addition for the second case under undersaturated and oversaturated conditions[21] [Colour figure can be viewed at wileyonlinelibrary.com]

5.3 | Electrowinning of U-Pu onto inert solid cathode in LiCl-KCl eutectic melts

Transuranic elements (plutonium, neptunium, americium, and curium) have very low activity coefficients in liquid cadmium.[22,23] Therefore, they stabilize upon dissolution in LCC and can be assembled together with uranium. It is known that plutonium collected by LCC before saturation occurs forms the intermetallic compound $PuCd_6$, which accumulates in the lower part of the LCC. However, supposedly due to the vertical temperature gradient during slow cooling, $PuCd_6$ may be separated to form Pu.[24] As a rule, when using LCC, a complete separation of U and Pu at the cathode current density of 0.2 A/cm^2 cannot be achieved and uranium is also collected into LCC.[24] For the predominant reduction of plutonium at LCC, it is necessary to maintain a certain cathode current density. The density of the cathode current used to recover Pu is proportional to the concentration of Pu in the molten salt. In other words, the plutonium reduction current at LCC is controlled by diffusion of the plutonium ions. To avoid the appearance of uranium dendrite, it is necessary to maintain a high Pu/U ratio in the molten salt. In particular, a smooth release of plutonium was observed at Pu/U = 7.[25]

Depletion of plutonium in the molten salt leads to a decrease in the lithium content in it. Thus, by controlling the process parameters, it is possible to obtain a U-Pu product of various compositions at the cathode. Now, we put ourselves a question, is it possible to obtain Pu in the same way that is, based only on the process-regulation, abandoning completely the liquid cathode?

The answer to this question was provided by Sakamura et al,[26] where plutonium deposition was studied on the tungsten (W) electrode. In this work, the co-deposition of U-Pu was investigated on an inert solid cathode at various ratios of Pu^{3+}/U^{3+} concentrations and different cathode current densities. The concentration of U^{3+} in the eutectic electrolyte LiCl-KCl was varied, and the concentration of Pu^{3+} was kept constant. The standard potential of Pu^{3+}/Pu (−1.593 V) is more negative than the potential of U^{3+}/U (−1.283 V). The U^{3+} concentration was increased by adding the LiCl-KCl-UCl_3 salt (25.7 wt% U) in a stepwise manner, whereas the Pu^{3+} concentration was constant within 2.8 to 2.9 wt%.

Chronopotentiograms measured at different currents and different content of Pu^{3+} in salt are shown in Figure 6. At a current strength of 0.08 A, the electrode potential was kept below −1.6 V and metallic plutonium was deposited during all 500 seconds (Figure 6A). The potential surges above −1.6 V at the lower current values indicate a cessation of Pu evolution. The lower current strength results in the prolonged deposition of metallic U, rather than metallic Pu on the W cathode.

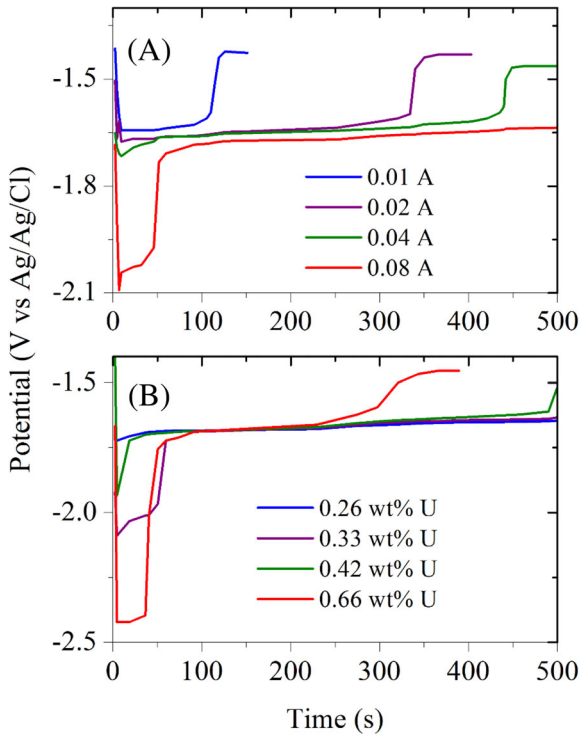

FIGURE 6 Chronopotentiograms on the W cathode (2 mm diameter) in the LiCl-KCl eutectic melts containing 2.8 to 2.9 wt% of Pu^{3+} and various concentrations of U^{3+} at 773 K: A, U^{3+} concentration is 0.33 wt%, current is 0.01 to 0.08 A; B, U^{3+} concentration is 0.26 to 0.66 wt%, current is 0.08 A[26] [Colour figure can be viewed at wileyonlinelibrary.com]

The galvanostatic electrolysis carried out at the current of 0.08 A showed that only at low concentrations (0.26 and 0.33 wt%) of U^{3+} in the salt metallic Pu is deposited on the W electrode during all 500 seconds (Figure 6B). At higher U^{3+} concentrations, an abrupt increase in the electrode potential above the value of −1.6 V in the considered time interval was observed. The potential surge led to the termination of the deposition of metallic Pu on the W electrode.

The results of the study showed that it is possible to deposit Pu along with U on a solid inert cathode provided that the concentration of U^{3+} in the salt does not exceed a certain limit. In other words, the precipitation of Pu and other actinides begins when the concentration of U^{3+} falls below the limit. To obtain the continuous deposition of Pu, it is necessary to ensure that during electrolysis the current increases in proportion to the increase in the surface area of the electrode. A continuous deposition of the Pu (together with U) at the cathode is difficult to maintain. Improving the anode can help to solve this problem.

The reduction of uranium and partially plutonium has been studied for a long time. One of the main reasons is the decrease in radiotoxicity during hydrochemical or pyrochemical processing of SNF. The latter method is more preferable because of the high radiation resistance of the saline solvent and the shorter cooling time.[27,28] A large number of studies have also been devoted to the reprocessing of metallic fuel from a fast reactor.[29-31] The purpose of such studies is usually to optimize the separation efficiency. However, minimizing the content of fission products is also important, especially lanthanides with high neutron capture. The electrochemical data for U-Cm actinides in LiCl-KCl melt still require refining.[23,32]

6 | MASS TRANSFER

6.1 | Kinetic model to simulate multispecies electrorefining in molten salt

To simulate electrorefining, a cell with a loaded salt electrolyte, an anode, and a solid or liquid cathode immersed in it was used. Uranium and transuranium elements, fission products of spent metal fuel, and noble metals are the objects of modeling. The model combines

electrochemical kinetics, thermodynamics, and transport. Based on the kinetic model developed by Seo et al,[33] the diffusion boundary layer thickness, transfer coefficients, and the difference between electrochemical potentials were calculated.

The transfer of ions in the molten salt is described by the Nernst-Planck equations:

$$\frac{\partial C_j}{\partial t} = -\nabla J_j. \tag{18}$$

$$J_j = -D_j \nabla C_j + C_j \cdot v - \frac{z_j F}{RT} D_j C_j \nabla \phi, \tag{19}$$

where C_j is the species concentration, J_j is the mass flux, D_j is the diffusion coefficient, v is the average speed of molten salt, z_j is the ion valence, and ϕ is the electrical potential.

When the convection coefficient can be isolated separately, Equation (18) can be replaced by a one-dimensional equation representing Fick's second law:

$$\frac{\partial C_j}{\partial t} = D_j \frac{\partial^2 C_j}{\partial x^2}. \tag{20}$$

With this representation, the movement of ions in the volume of the electrolyte is mainly determined by convection, and in a thin boundary layer—by diffusion. The boundary conditions in the form of the mass of the dissolved or precipitated substance are determined using Faraday's law. The concentration-dependent currents at the cathode and anode are determined using the charge transfer coefficient, overvoltage, and species mole fractions at the electrode. The equilibrium potential of the species is expressed through the activity, standard potential, activity coefficient for species, and reaction quotient. In the Nernst equations recorded at the electrodes, the activities of species are expressed through the corresponding concentrations and specific activity coefficients in the molten salt and in the liquid Cd electrode. Equation (20) is discretized and extended by semi-implicit methods to find the concentrations of the species. This makes it easier to find solutions.

In the Cd electrorefining process, the electrode plays a double role. At the first stage of this process, it serves as a cathode in which U, Pu, and MA are deposited. The second stage of the process denotes the deposition of U mainly and that of Pu, to a lesser extent, on a solid (most often metallic) cathode. In this case, the cadmium electrode serves as an anode.

The change in the composition of U and Pu in liquid Cd is shown in Figure 7. On the whole, the model reproduces quite well the decrease in the concentration of U and Pu, which is caused by the oxidation of these metals with the subsequent release of ions into the molten salt. Nevertheless, the rate of Pu depletion in liquid Cd in the model is higher than in the experiment. Therefore, at the final stage of modeling, the Pu concentration in the model is ~20% lower than in a real experiment.

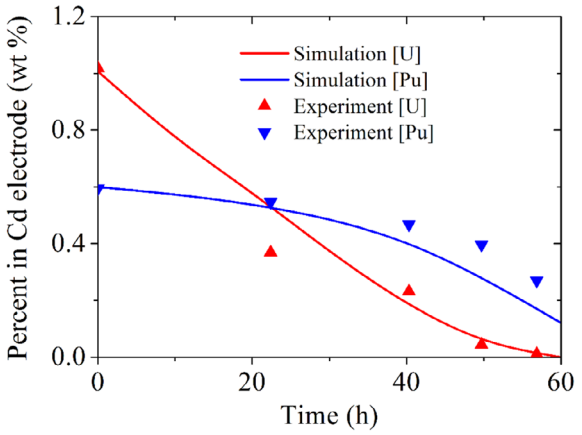

FIGURE 7 Weight percentages of U and Pu in the Cd electrode, compared with the experimental results[33] [Colour figure can be viewed at wileyonlinelibrary.com]

Figure 8 shows the change in the concentration of U and Pu in the volume of molten salt. These time dependences have the same tendencies and reflect quite acceptable agreement between the calculated and experimental data. The Pu concentration in the electrolyte volume steadily increases; however, after 50 hours, the rate of replenishment of the melt with Pu^{3+} ions decreases. After 50 hours, the U concentration in the molten salt of the model becomes higher than in the experiment. The

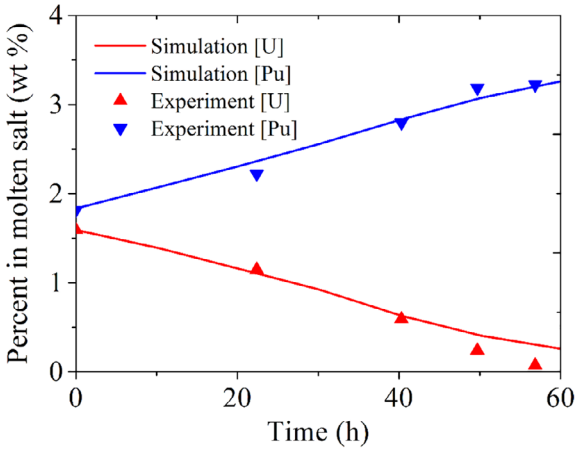

FIGURE 8 Weight percentages of U and Pu in molten salt bulk, compared with the experimental results[33] [Colour figure can be viewed at wileyonlinelibrary.com]

diffusion coefficient of Pu^{3+} (1.6 10-5 cm^2 s^{-1} at 733 K) in the LiCl-KCl melt and its activity were determined.[34]

The model can be refined by taking into account the presence of Np and Am in liquid Cd. This should help to improve the agreement with the experimental Pu behavior. An insignificant dependence of the characteristics of electrorefining observed in the liquid Cd electrode on the width of the diffusion layer and the difference between standard potentials was found.

6.2 | Recovering uranium with a cadmium-lithium anode

After the electrorefining, the waste salt may contain up to 10 wt% of U or Pu. This salt should be replaced with a fresh salt to avoid the accumulation of fission product chlorides. You can refresh the salt melt without removing it from the electrolytic cell. For this purpose, an electrorefining session should be carried out using a Cd-Li anode and without changing the solid cathode. During this procedure, heavy metals will be recovered by the cathode.

Kobayashi et al[35] preformed the electrorefining with a Cd-Li anode, both experimentally and theoretically. The experimental study was carried out in a glove box, where the electrolyzer was placed. The experimental equipment for the study of electrical transport was very similar to the equipment used in Iizuka et al[15] (Figure 9). The box was filled with high-purity argon gas. The crucible body was made of mild steel. A Cd-Li (4.41 wt% Li) anode, a solid low-carbon steel cathode, an Ag/Ag^+ reference electrode, and a stirrer were placed into the crucible. The anode crucible was made of zirconium dioxide. The bottom of the solid cylindrical cathode rested on a zirconium plate to avoid uranium deposition there. The upper part of the solid cathode was covered with an aluminum oxide tube. Thus, the effective cathode area was formed only by the lateral surface of the cylinder. The material transport of U^{3+} and Pu^{3+} ions was improved by the rotation mechanism (20 rpm), to which the cathode was connected. The collection of uranium deposits was carried out using a trapping tray located under the cathode. The Cd pool in the salt phase (LiCl-KCl) was mixed with a two-impeller stirrer.

The working temperature of the refining process was 773 K. At this temperature, the activation and redox processes occur quickly on the electrodes and equilibrium is established. Therefore, the Nernst equation can be used to represent the anode potential in terms of the activities of the components (U^{3+} and Li^+) at the anode.

The oxidation of lithium created by the Cd-Li anode leads to the fact that the potential of the anode (E^a) becomes more negative than the redox potential of $U^{3+} + 3e^- = U$ (E^0_U). Therefore, U^{3+} is restored at the Cd-Li anode. This electrochemical process is expressed in the presence of a negative anode current (J^a_U). In this case, the lithium anode current (J^a_{Li}) turns out to be even greater than the total anode current (J^a). As a component, this current includes the current addition J^0_{Li} from the component Li^0 dissolved in the salt without oxidation. The current J^0_{Li} arises due to the dissolution and the structuring of the Li^0 component, in the salt without oxidation. This current appears when the interface is displaced to the right due to the depletion of the bulk electrolyte in atomic Li due to the tendency of these neutral atoms to form clusters in the molten salt.[36]

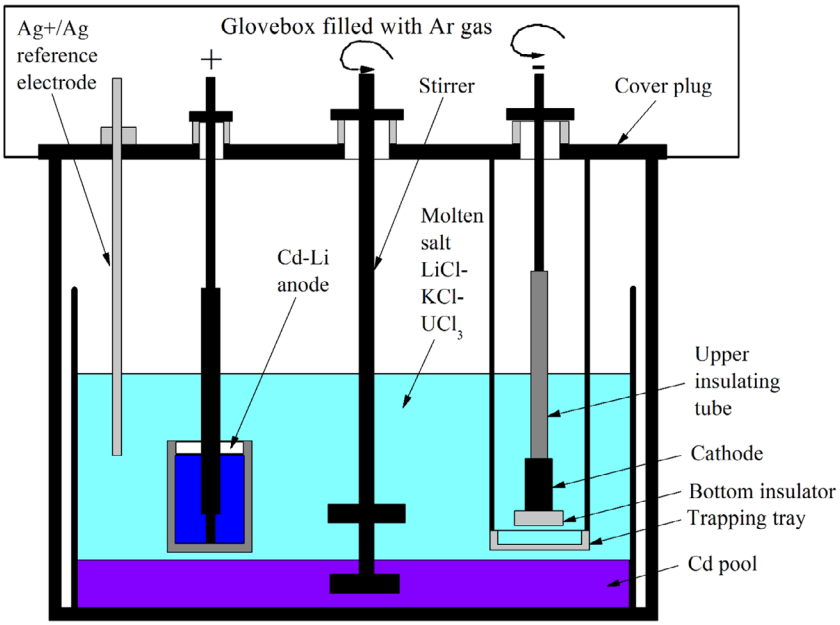

FIGURE 9 Experimental apparatus for the electrotransport with the Cd-Li anode[15] [Colour figure can be viewed at wileyonlinelibrary.com]

In the course of the experiment, the U^{3+} concentration in the salt melt was reduced from 1.38 wt% to less than 0.01 wt%. At high U^{3+} concentrations (1.38 wt% $< C_{U3+} <$ 10 wt%), this heavy ion is easily removed from the melt during electrorefining. Therefore, taking the initial value of the U^{3+} concentration to be equal to10 wt%, Kobayashi et al[35] believe that the degree of removal of U^{3+} from the melt is 99.9%. However, this does not mean that all 99.9% of the recovered uranium is deposited on a solid cathode. The calculation of the mass balance showed that a noticeable part of uranium is also reduced at the anode. The uranium deficit was calculated with respect to the cathode with ideal efficiency, that is, at which 100% of U^{3+} is deposited. Electrotransport experiments were performed under different current conditions. The experimental data were obtained at the initial U content in the salt of 0.66, 0.99, 1.38 (wt%), and anodic current of 3.50, 2.35, 1.19 (A), respectively.

At high concentrations of U in the salt, the experimental values of the uranium deficit are in good agreement with the calculated values obtained at the diffusion layer thickness near the anode $\delta = 0.050$ cm under the assumption that the diffusion coefficients (D^0_{Li} and D^+_{Li}) of electrically neutral Li atoms and Li^+ ions in the salt melt are equal. Due to the interaction of Li^0, which penetrates from the Cd-Li anode into the salt melt, with other ions in the salt, the diffusion coefficient of Li^0 can be higher than that of Li^+. However, the situation changes when the concentration of U in the salt is low. In this case, the best agreement between the calculation and experiment is achieved at half the thickness of the diffusion layer, but maintaining the equality of the diffusion coefficients of lithium atoms and ions. However, a 2-fold increase in D^0_{Li} in comparison with D^+_{Li} also brings the calculated value of the deficit U closer to the experimental value even if the value of the diffusion layer thickness remains equal to 0.050 cm.

The extraction of uranium from the molten salt in the electrolyzer with a Cd-Li anode can be simultaneously performed in two ways: as a result of electrochemical reduction at the cathode and due to chemical interaction with Li^0. The strong current is J^a_{Li}, which is even higher than the total current due to the fact that the current J^a_U flows in the opposite direction and its values are considered negative. Both of these currents decrease with time, while the total current J^a remains almost unchanged. The current J^0 associated with the dissolution of Li atoms in the molten salt is a noticeable value of the current generated by Li^+ ions, that is, . J^a_{Li}.

Thus, the cathodic uranium deficiency was created in two ways: (a) using the electrochemical deposition of U^{3+} at the anode and (b) dissolution of atomic lithium (Li^0) in the eutectic LiCl-KCl salt. The latter option assumes the concomitant reduction of U^{3+} by Li^0. The calculations performed showed that both of these mechanisms are highly probable if the diffusion coefficient of Li^0 in the salt is greater than that of U^{3+}.

6.3 | Prediction of partitioning of plutonium from curium in a pyrochemical process

The ^{244}Cm isotope has an extremely high rate of spontaneous neutron emission, which is approximately four orders of magnitude higher than that of ^{240}Pu and nine orders of magnitude higher than that of ^{239}Pu. Therefore, according to the Cm content in a functioning electrolyzer, it is advisable to monitor the effectiveness of protection against radioactive radiation. If during the processing, the ratio between the Pu and Cm contents is not violated, then the neutron balance method can be applied to the entire pyrochemical recycling. In other words, the Pu content in a loaded electrolyzer can be determined according to the high radiative activity of neutrons for ^{244}Cm. To fulfill the principle of the neutron balance, the behavior of plutonium and curium must be identical during the entire extraction process and at the stage of product recovery. However, it is extremely difficult to quantify experimentally the concentration of ^{244}Cm, when the goal is to detect the amount of Pu. This is due to the fact that the content of Cm in the molten salt, as a rule, is below the limit of its detection.[33] However, the anode dissolution of SMF, the effects of the transfer of its components in molten salt electrolytes, as well as cathode deposition can be studied by calculation.

The Cm deposition on a solid cathode in the LiCl-KCl melt was studied by Gonzalez et al.[37] Assuming that the exchange current density includes effectively the activity coefficient and the molar fraction of CmCl and following the Butler-Volmer equation, one can present the slope in the cyclic voltammetry characteristic in the following form:

$$slope = i^0_0 A \left(x^{ox}_b\right)^{\alpha} \frac{nF}{RT}, \tag{21}$$

where i^0_0 is the standard exchange current density (A cm^{-2}), A is the surface area (cm^2), x^{ox}_b is the mole fraction of the oxidized species in the bulk, α is the transfer coefficient, and n is the number of electrons transferred.

According to the experimental data obtained in molten LiCl-KCl-$CmCl_3$, presented in the form of cyclic voltammetry at three different sweep potential rates of 1.0, 0.7, and 0.5 V s^{-1}, the authors determined the slopes in the voltage dependencies of the current and found the

average current density i_0^0 of 0.47 A/cm^2 for Cm^{3+}. A plutonium mass deposited on the cathode, sensitivity of cathode potential (vs Cl_2/Cl^-) to standard exchange current density, and Pu/Cm ratio in the molten salt (all as a function of time) were calculated, using standard exchange current densities (i_0^0) for U^{3+} and Pu^{3+} in LiCl-KCl (1.0 and 0.8 A/cm^2, respectively) as well as the found current density for Cm^{3+}.[38] We have determined that the change in value y, which is equal to the Pu/Cm ratio, with time obeys the following analytical relationship with high accuracy:

$$y = y_0 + A\exp(R_0 x), \tag{22}$$

where time x is expressed in hours.

The temporal behavior of y together with the parameters of Equation (22) is shown in Figure 10. It can be seen from Figure 10 that the Pu/Cm ratio in the melt of the LiCl-KCl salt mixture decreases during electrorefining due to the deposition of Pu at the cathodes.

The equilibrium reduction potential of Cm is quite negative, therefore, Cm should not be present in any significant concentrations in Pu deposits at both (steel and cadmium) cathodes. In the calculations, it is assumed that Cm does not form metal alloys with U or Pu. When the ratio Pu/Cm > 100 is maintained in a SNF (which is always true in reality), Cm is not deposited on the cathode and the curium balance is not maintained during the pyroprocessing. Therefore, the Cm content does not track Pu at the electrorefining cathode. Other sensors must be used to determine the Pu mass, and additional precautions must be taken.

The modeling of electrochemical dissolution of spent fuel has been implemented using various methodologies.[39-48] At first glance, it seems that the measurement of the amount of dissolved elements in the molten salt can be used to control the electrorefining process. It is of interest to carry out a nondestructive testing during the pyroreprocessing of SMF by counting neutron emissions. This could provide a fairly simple solution to the problem of tracking the mass of plutonium during the electrorefining. However, the use of the balanced neutron radiation approximation proved to be unsuitable for this purpose due to the lack of congruence ratio with respect to Pu/Cm in the molten LiCl-KCl salt mixture and on the cathode.[37]

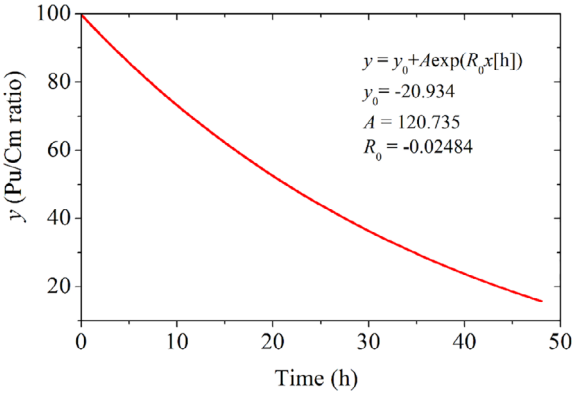

FIGURE 10 Averaged Pu/Cm ratio over the Cm^{3+} current densities of 0.47, 0.8, and 1.6 A/cm^2 in the molten salt for a total cell current of 350 A [Colour figure can be viewed at wileyonlinelibrary.com]

7 | ANODIC DISSOLUTION

7.1 | Anodic behavior of U, Zr, and U-Zr alloy in molten LiCl-KCl eutectic

The high efficiency of electric cleaning was demonstrated by SMF electrolysis with a burnup of 2.5 at.%.[49] The degree of dissolution of actinides was U: 98.9%, Pu: 99.8%, Np: 99.0%, Am: 98.9%. At the same time, most of Zr and noble metals were concentrated in the anode residues. Moreover, the alternation of layers of porous Zr with a layer of noble metals was found.

Murakami et al[49] studied the anodic dissolution of U, Zr, and the U-Zr alloy and evaluated the thickness of the diffusion layer at the metal-salt melt interface. The work is based on using the results of anode polarization of U, Zr, and the U-Zr alloy in the molten eutectic LiCl-KCl. A simplified zirconium anode dissolution modeling in the eutectic LiCl-KCl can be performed using a single parameter, that is, the δ-thickness of the diffusion layer at the boundary of porous zirconium and of the molten salt.[50] It is not possible to experimentally determine this parameter. The anode potential E_a is determined from the Nernst equation:

$$E_a = E_i^0 - \frac{RT}{z_i F}\ln\left(\frac{1}{\gamma_i^s X_i^{a/s}}\right). \tag{23}$$

The charge flux density, determined by ions of type i, at the anode is defined as:

$$i_i^a = z_i F D_i^s \frac{X_i^{a/s} - X_{i,b}^s}{\delta_{i,a}^s}, \tag{24}$$

here γ_i^s is the concentration of i ions in the salt, $X_i^{a/s}$ is the concentration of i ions at the anode/salt interface, z_i is the number of electrons participating in the reaction, and $\delta_{i,a}^s$ is the diffusion layer thickness for species i at the

salt-solid anode interface. The activation overpotential η_i is calculated according to Equation (24) if the value of current i_i^a is known. A porous zirconium layer is a barrier for the dissolution of actinide ions.

The activation of polarization for each component i can be taken into account based on the use of the Butler-Volmer equation. The partial anode current created due to the motion of i particles with the participation of z_i electrons is defined as:

$$i_i^a = i_i^{0,a}\left[\exp\left(-\frac{(\alpha_i z_i)F\eta_i^a}{RT}\right) - \exp\left(\frac{(1-\alpha_i)z_i F\eta_i^a}{RT}\right)\right], \quad (25)$$

where $i_i^{0,a}$ is the exchange current density i_i^a during anodic dissolution and α_i is the different transfer coefficient.

Each component has its own transfer coefficient α_i gain by determining the corresponding polarization using the following two equations.

Tafel equation:

$$\eta_i^a = \frac{RT}{(z_i\alpha_i F)}\ln\left(i_i^{0,a}\right) - \frac{RT}{(z_i\alpha_i F)}\ln\left(i_i^a\right). \quad (26)$$

Allen-Hickling equation:

$$\ln\left[\frac{i_i}{1-\exp(z_i F\eta_i^a/(RT))}\right] = \ln\left[i_i^{0,a}\right] - \frac{\alpha_i z_i F}{RT}\eta_i^a. \quad (27)$$

The calculated curve of the anode polarization of the U-Zr alloy in molten LiCl-KCl-UCl_3 in comparison with the corresponding experimental curve is shown in Figure 11.[51] The calculated data presented in Figure 11 were obtained at the diffusion layer thickness $\delta = 0.0004$ cm. The calculated curve $i(E)$ is in a satisfactory agreement with the corresponding experimental curve. However, the obtained experimental curve has some peak features at 0.9, 0.5, and 0.3 V, which can be attributed to the formation of redox couples Zr^{2+}/Zr^{4+} and U^{3+}/U^{4+}. The formation of such couples is associated with oxidation of metallic Zr and U at higher anode potentials. A possible formation of such products was not predicted by calculation.

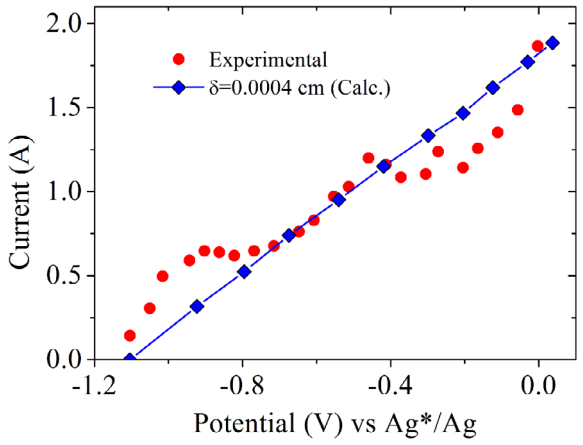

FIGURE 11 Anode polarization of the U_6Zr alloy calculated at $T = 808$ K and the corresponding experimental curve obtained at 773 K[51] [Colour figure can be viewed at wileyonlinelibrary.com]

In this case, two experimentally observed cyclic voltammograms show two anode peaks related to U and Zr dissolution, respectively. The wide shape of the first peak is due to the resistive effect of the working electrode. The experimental data obtained in Reference 48 show that the studied metals (U, Zr) and the U-Zr alloy have close values of the thickness of the diffusion layer. The relation between the thickness of the diffusion layer, the density of the exchange current, and the transfer coefficient for U, Zr, and U-Zr is found. Further electrochemical studies are needed to understand the co-dissolution of zirconium during the SMF electrorefining.

7.2 | Treatment process for anode residue from electrorefining of SMF

Since the restoration of zirconium requires considerable time, it is not completely restored and accumulates in the electrorefiner. The zirconium remaining at the cathode requires an increase in the operating temperature during the cathode treatment operation. Therefore, it is desirable that zirconium remains on the anode. Iizuka et al[52] proposed a quick process of extracting the anode residue. This process is divided into two stages.

The first one is the addition of a chloride solvent in the form of $CdCl_2$, which leads to the dissolution of the remaining actinides in the anode residue. During the second stage, the chlorides are removed by high-temperature distillation.

As a result, a compacted deposit remains at the anode, which must be disposed of, and the chlorides of the recovered actinides are returned for repeated electrorefining.

In Reference 52, a two-stage experimental study was carried out on the refining of the anode residue obtained as a result of conventional electrorefining of the U-Zr alloy. At the first stage, the deposited uranium and zirconium were dissolved in the LiCl-KCl salt melt due to the oxidation, which was initiated by the addition of $CdCl_2$ to the used electrolyte. In this case, the anode basket with the residue was placed in the molten eutectic solvent LiCl-KCl at 773 K. The second stage of the procedure consisted in evaporating the product obtained in the first stage by heating it with an induction heater under

vacuum to 1473 K for 1 hour. This operation allowed distillating the chlorides. Then, the obtained anode residue was heated to 1673 (4 hours) and to 1773 K (0.5 hour) for metal consolidation in an argon atmosphere. The procedure was completed by slow cooling of the anode residue. This study used two types of metal alloys that underwent an electrorefining operation. The first type was represented by a pure U-Zr alloy, which did not contain any other elements. The second type of U-Zr alloy contained a small amount of cerium, neodymium, molybdenum, and palladium to simulate the elements of fission products.

Considerable time is required (25-30 hours) to achieve stable uranium concentration values after the first introduction (50 hours after the start of electrorefining) of $CdCl_2$ into the molten salt. This is due to the difficulty of UCl_3 passing through the porous anode residue. The second addition of $CdCl_2$ (after 100 hours) almost does not change the concentration of uranium. The concentration of zirconium after the first and second addition of $CdCl_2$ quickly reaches a maximum and then drops almost to zero. This behavior of the Zr concentration indicates that the very first addition of $CdCl_2$ leads to the complete dissolution of the uranium present in the deposit. The presence of uranium decay products in the anode residue has practically no effect on the nature of the change in the considered concentrations.

The study[52] showed that the rapid increase in the rate of uranium concentration caused by the addition of $CdCl_2$ persisted for the first 4 hours. Over the past 4 hours, this indicator decreased due to the dissolution of zirconium, as the rate of addition of $CdCl_2$ became too high. Therefore, it is necessary to monitor changes in U concentrations during this operation, for example, using the electroanalytical control method.[53,54]

After distillation, the chlorine content in the anode residue was from 2000 to 5000 ppm. As a result of a two-stage processing of the anode residue, the uranium content in it decreased to 0.04% to 0.20%. This value is quite low since the acceptable recovery factor for uranium is 99.5%. Adding the anode residue treatment, using $CdCl_2$ after the pyrometallurgical processing will not reduce productivity and will not significantly increase the cost of the electrorefining process.

Iizuka et al[53] presented an even more detailed study of the dissolution process of the soluble anode material during the SMF electrorefining than in Reference 49. Electrorefining, which is carried out in the LiCl-KCl eutectic at 773 K, is considered to be a necessary operation in the reprocessing of SMF.[55,56] During this process, a chemical equilibration of SMF (U-Pu-Zr) with a stoichiometric amount of $CdCl_2$ is proposed. This procedure was investigated using cyclic voltammetry, chronoamperometry, and convolution voltammetry.[51] After the equilibration, UCl_3 and $PuCl_3$ were formed together with the chlorides of fission products in the molten salt. The diffusion coefficient of U_3 in the melt was calculated (2.9×10^{-5}-3.3×10^{-5} cm^2 s^{-1}). The electrode kinetics were studied by the behavior of Zr^{4+}/Zr^{2+} redox couple in LiCl-KCl-$ZrCl_4$.

7.3 | Irradiated metallic fuels in LiCl-KCl melt

Murakami et al[49] performed the electrorefining of metallic fuel with the composition of U—19 wt% Pu—10 wt% Zr, irradiated in a fast neutron reactor and after a burnup of ~2.5 at.%. The study of the behavior of actinides in a traditional molten salt (LiCl-KCl) was carried out using an Ag/AgCl reference electrode. Potentiostatic 1, galvanostatic, and potentiostatic 2 electrolyses were performed with different initial fuel compositions. The first two electrolyses were performed at −1.0 V vs Ag/AgCl, and the latter at −1.04 V vs Ag/AgCl. In all three experiments, solid cathodes were used.

The increase in the charge passed through the electrolyzer resulted in the decrease in the concentration of U, while the concentration of transuranic elements (Pu, Np, and Am) increased. This is due to the fact that U is reduced on solid cathodes, and transuranic elements accumulate in the molten salt. Moreover, some of them dissolve as a result of the exchange reaction with U^{3+} present in the melt.

The concentration of alkalis and alkaline earth elements such as Na, Cs, and Ba increases in the molten salt as the amount of missed charge increases. This can be seen from Figure 12, which shows the dependence of the concentration of Cs and Ba in the molten salt depending on the amount of charge passed through the electrolyte. It should be noted that the progress of the anode dissolution is not the determining factor in the dissolution of alkali and alkaline earth metals. Immersion of the initial anode content in the corresponding electrolyte without electrolysis showed that the concentrations of Cs, Ba, and Na increase. This indicates that the dissolution of alkali and alkaline earth metals proceeds according to the reactions:

$$3A + U^{3+} \rightarrow 3A^{+} + U \ (A: \text{Cs and Na}), \quad (28)$$

$$3Ba + 2U^{3+} \rightarrow 3Ba^{2+} + 2U. \quad (29)$$

It was also found in Reference 49 that the concentration of rare earth elements (La, Ce, Pr, Nd, and Y) in the

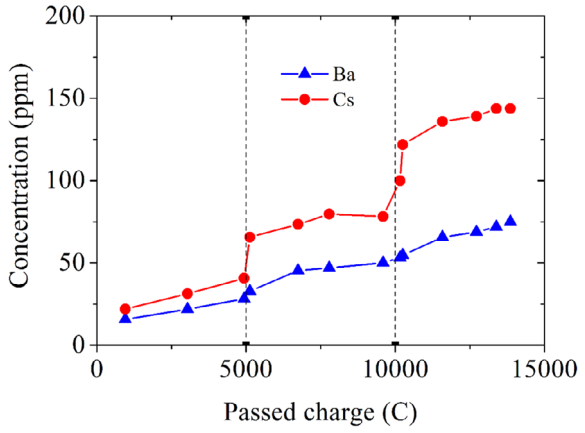

FIGURE 12 Cs and Ba concentrations in the molten salt during electrorefining. The dashed lines separate the experiments with different initial contents of Cs and Ba[49] [Colour figure can be viewed at wileyonlinelibrary.com]

molten salt increased as the charge passed, which is reflected in Figure 13 for Ce and Nd. However, the concentration of rare earth elements also increased after immersing the anode basket with the starting material in the corresponding molten salt without electrolysis. This follows from the exchange reaction of rare earth elements with U^{3+}, namely:

$$RE + U^{3+} \rightarrow RE^{3+} + U\,(RE: La, Ce, Pr, Nd \text{ and } Y). \quad (30)$$

Still, during electrolysis, rare earth elements do not completely dissolve. A noticeable number of them are found in the anode residues. There is an opinion that some rare earth elements form alloys with noble metals upon irradiation.[57,58] Such elements can be present in the anode residues, especially when the co-dissolution of Zr at the anode is limited.

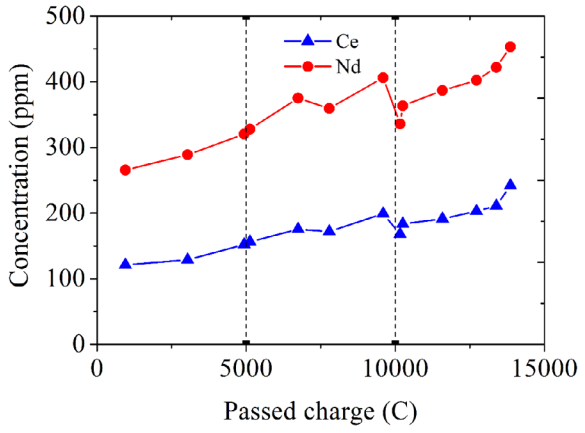

FIGURE 13 Ce and Nd concentrations in the molten salt during electrorefining. The dashed lines separate the experiments with different initial contents of Ce and Nd[49] [Colour figure can be viewed at wileyonlinelibrary.com]

Despite the fact that the anode potential was maintained below the dissolution potential of metallic zirconium, a part of the Zr was anodically dissolved. A part of Zr reacted with actinides, rare earth elements, alkaline and alkaline earth elements. As a result, metallic Zr was detected both on the anode and on the cathode, and they also partially accumulated on the bottom of the crucible. Most of Zr and noble metals remained in the anode residues.

8 | DISCUSSION

The experimental electrorefining, similar to that reported the works,[2,26,49] was carried out at the Institute of High-Temperature Electrochemistry, Ural Branch of the Russian Academy of Sciences, on an enlarged water-cooled laboratory electrolyzer made of stainless steel grade.[59] The anode basket was made of the PM (pure molybdenum without additives) grade metal molybdenum wire (GOST-27266-87). Metallic uranium was loaded into the basket in the form of separate glazing beads with an average length of 40 to 70 mm, a width of 5 to 10 mm and a thickness of 2 to 3 mm. The anode current density did not exceed 0.01 A/cm^2. The refining process was carried out in a crucible-container made of glassy carbon GC-2000. The crucible was loaded with the calculated amount of uranium-containing electrolyte, if necessary, it was diluted with an eutectic mixture of 3LiCl-2KCl. Cylindrical rods made of metallic molybdenum of the PM grade and alloy XH62M were used as the cathode.

To ensure the safety of the electrorefining process, the oxidation of dispersed depleted uranium should be excluded. The fact is that uranium powder, as a pyroform material, can be ignited in air when exposed to oxygen. In principle, there are two ways to make the process of uranium electrolysis safer. The first option is based on conducting electrolysis in an inert gas medium. Most often, argon is chosen for this, as the cheapest inert gas. The argon pressure in the working volume should be slightly higher than the atmospheric one. A dry, inert environment will prevent the formation of salt hydrates that may form due to the presence of water in the air and will help to keep the salt clean. A possible inert gas escape outside the installation is the disadvantage of this method, if this is not specifically provided by the design of the electrolyzer. The second way to design safely the cell is to conduct electrolysis under not too high vacuum conditions. In this case, hazardous gaseous substances

are trapped inside the cell. However, this method of protection against the ingress of oxygen into the apparatus is not entirely reliable, because any leaks formed will pull oxygen into the system.

We would like to draw your attention to some general details that characterize the process of electrorefining of SNF obtained as a result of the operation of thermal and fast reactors. First of all, it is appropriate to analyze the influence of various factors associated with the experimental conditions on the results of electrorefining of SNF in the molten eutectic mixture 3LiCl-2KCl. This electrolyte has been most often used recently for the electrorefining of SNF. The following parameters can be recommended as response factors: the current yield of the deposited metal, the morphology of the deposit obtained at the cathode, and the capture of the electrolyte by the cathode deposit. The influence of the cathode current density, the temperature of the process, the cathode material, the concentration of uranium in the electrolyte and the specific amount of passing electricity can be named variable parameters that change the electrorefining process.

Let us perform the above analysis using the Mo cathode. In the course of experiments at temperatures of about 500°C and a uranium concentration of ~7 wt% at a reduced cathode current density (0.05 A/cm^2), a dense compact deposit is formed on the cathode. It is not possible to remove it from the molybdenum cathode. In this case, the CE is close to 100%, and the capture of the electrolyte by the cathode deposit is about 7%. The chemical purity of the obtained metal is quite consistent with the anode material.

The U concentration in the electrolyte affects the structure of the cathode deposit. The most positive results can be obtained when the U concentration in the melt is maintained above 5 wt%. Then, at a cathode current density of 0.1 to 0.4 A/cm^2 and at the temperatures differing from 500°C ± 10°C, alpha-uranium with rhombic syngony is formed at the cathode. However, even under such conditions, a dense, compact deposit is formed on the cathode only at the initial stage. An increase in the duration of electrolysis leads to the formation of a dendrite-lamellar structure, organized by force fields. The optimal specific amount of electricity, excluding the formation of needle-lamellar deposits, at a current density of 0.4 A/cm^2 is 0.5 Ah/cm^2. An increase in the current density up to 0.6 A/cm^2 facilitates the removal of the deposit from the cathode, but causes an increase in the capture of electrolyte up to 18.5%. A decrease in the concentration of U in the electrolyte below 4 wt% at the same current densities, also changes the morphology of cathode deposits, leading to the growth of dendritic structures. However, the content of impurities in the cathode product, as well as the CE, which is usually 85% to 90% do not contribute greatly to the morphology and structure of cathode deposits.

A radical change in the morphology of the cathode deposit at a temperature of about 500°C occurs when the cathode current density rises to 0.6 to 0.8 A/cm^2. In this case, the deposit is acicular and tends to come closer to the anode. If a large specific amount of electricity is passed in this mode, then the CE may decrease. This is due to the presence of contact between the cathode and the anode through the formed needles on the bath. However, even at such current densities, the electrolyte capture does not exceed 30%.

Uranium deposited on the solid cathode of an electrolytic refiner contains salt, which accompanies the metal from the electrolyte. Therefore, to obtain pure metallic uranium, further processing of this deposit is required. This operation must be carried out in an inert atmosphere and with real spent fuel on an industrial scale.

The main difference between the work presented in Reference 59 and the majority of works on the electrorefining of the SMF is the absence of an intermediate electrode in the form of liquid cadmium. This is due to the fact that metallic uranium with a purity of at least 99.5% and not the U-Pu alloy was loaded into the anode basket. One of the objectives of the study was to determine the optimal specific amount of electricity, excluding the formation of acicular-plate deposits on the cathode. The formation of alpha-uranium with rhombic syngony was achieved at a uranium concentration in the melt above 5 wt% and at a current density of 0.1 to 0.4 A/cm^2.

The process of uranium deposition in the LiC1-KCl melt looks like electrochemical deposition with controlled diffusion.[60] In this case, the formation of a diffuse field of the deposited ions, in which the protrusions grow in the direction of increasing concentration, causes the appearance of dendrites. During the deposition, the concentration profile changes periodically. This is due to a ripple in the current that causes fluctuations in the concentration. These vibrations, in turn, lead to the periodic relaxation of the diffusion field and cause a decrease in the growth of dendrites.[61] Periodic short concentration cycles between the anode basket and the walls of the refiner promote the formation of denser cathode deposits, that is, the level of the dendriticity is reduced.

A high concentration of dissolved ions and a significant effective gradient of the electric potential at the crystal-melt interface are necessary for the stable growth of deposits on the cathode.[62] This rule should be followed to obtain a dense deposit on a solid cathode.

Zirconium has a more positive dissolution potential than actinides.[63] Zirconium, which is a part of SNF, dissolves at the anode and is reduced at the solid cathode as

a U-Zr alloy. It can also deposit on the walls of the refiner. During the electrorefining, the amount of dissolved Zr should be minimized. This is due to the fact that Zr and particles of noble metals must be periodically removed from the refiner. Therefore, certain efforts are being made to reduce the joint dissolution of Zr.[64]

The presence of other actinides (except for U and Pu) and fission products in the irradiated fuel significantly reduces the controllability of the electrorefining process. The formation of their chlorides and the anodic dissolution of these elements, followed by the diffusion of the ions that appear, cause fluctuations in electrical parameters and destabilize the refining process. Noble metals are also involved in this process. In the course of such electrolysis, intermetallic compounds are formed. Therefore, it is extremely difficult to adjust the process for the deposition of a specific actinide, alkali, alkaline earth metal, as well as a rare earth element or a noble metal. To improve the electrorefining process, new experimental and theoretic studies are required.

9 | CONCLUSIONS

All works analyzed are united by a single global goal. Creation of an industrial-scale electrorefining unit is a far-reaching design. To start the production process of SNF or SMF reprocessing, first of all, it is necessary to grind the fuel cells to a size suitable for insertion into the anode basket of the electric refiner. In laboratory experiments, unirradiated metallic fuel is more often subjected to electrorefining, than the irradiated one, and, as a rule, the daily yield is not exceeding 10 kg of heavy metal. In a similar industrial-scale process, irradiated metallic fuel is recycled to obtain a desired yield of 200 kg of heavy metal per day. So far, neither industrial, nor laboratory-scale electrolytic cells have been developed for the reprocessing of more complex types of SNF fuel, such as metal hydride, metal-aluminum or metal-silicon alloys, as well as fuels with aluminum cladding, by the electrometallurgical method.

A fuel used in nuclear power can be reprocessed, that is, fissile material can be removed. A fresh fuel can be created for existing and future nuclear power plants. The creation of a reprocessing industry in the nuclear industry means that a spent fuel is treated as a resource and not as a waste. One of the main tasks is the recovery of unused plutonium, including the production of U-Pu and Zr-U-Pu alloys. The recovered Pu and U are destined for use in fuel cells and thus it becomes possible to close the fuel cycle. This makes it possible to obtain 25% to 30% more energy than by traditional production at nuclear power plants. In addition, the volume of highly radioactive waste material is reduced to one-fifth. The fact that the level of radioactivity in the waste after reprocessing is much lower and declines much faster than in the spent fuel itself is of great importance. For the full implementation of this project, fast reactors are needed. A complete reprocessing of SNF changes the strategy of fuel resources. The source of fuel is not only the used fuel of today's reactors, but also the large stocks of depleted uranium produced in enrichment plants. Uranium mining will become less important due to the fact that nuclear waste will be used only as a subject of reprocessing. The products of this reprocessing can serve as fuel for fast reactors, which will burn all long-lived actinides.

ACKNOWLEDGEMENTS

This work was supported by the State Atomic Energy Corporation Rosatom (State Contract No. H.4o.241.19.20.1048 dated April 17, 2020, identifier 17706413348200000540).

DATA AVAILABILITY STATEMENT

The data that support the findings of this study are available from the corresponding author upon reasonable request.

ORCID

Alexander Y. Galashev https://orcid.org/0000-0002-2705-1946

REFERENCES

1. Rodríguez-Penalonga L, Soria BYM. A review of the nuclear fuel cycle strategies and the spent nuclear fuel management technologies. *Energies*. 2017;10:1235.
2. Uozumi K, Iizuka M, Kato T, et al. Electrochemical behaviors of uranium and plutonium at simultaneous recoveries into liquid cadmium cathodes. *J Nucl Mater*. 2004;325:34-43.
3. Willit JL, Miller WE, Battles JE. Electrorefining of uranium and plutonium - a literature review. *J Nucl Mater*. 1992;195:229-249.
4. Kim JH, Alameri SA. Harmonizing nuclear and renewable energy: case studies. *Int J Energy Res*. 2020;44:8053-8061.
5. Vavilov S, Kobayashi T, Myochin M. Principle and test experience of the RIAR's oxide pyro-process. *J Nucl Sci Technol*. 2004;41:1018-1025.
6. Galashev AY, Ivanichkina KA, Zaikov YP. Computational study of physical properties of low oxygen UO_{2-x} compounds. *J Solid State Chem*. 2020;286:121278.
7. Galashev AY, Manzhurov AI, Zaikov YP. Computer modeling of electrochemical processing of waste nuclear fuel. *Int J Energy Res*. 2020. https://doi.org/10.1002/er.5462.
8. Galashev AE, Stakhanov VV, YuP Z. Modeling the design of an electrolytic cell for reprocessing spent nuclear fuel. *High Temp*. 2020;58:342-351.
9. Sofu T. A review of inherent safety characteristics of metal alloy sodium-cooled fast reactor fuel against postulated accidents. *Nucl Eng Technol*. 2015;47:227-239.

10. Hofman GL, Walters LC, Bauer TH. Metallic fast reactor fuels. *Prog Nucl Energy*. 1997;31:83-110.
11. Carmack WJ, Porter DL, Chang YI, et al. Metallic fuels for advanced reactors. *J Nucl Matr*. 2009;392:139-150.
12. Koyama T, Iizuka M, Shoji Y, et al. An experimental study of molten salt electrorefining of uranium using solid iron cathode and liquid cadmium cathode for development of pyrometallurgical reprocessing. *J Nucl Sci Technol*. 1997;34:384-393.
13. Paunovic M, Schlesinger M. *Fundamentals of Electrodeposition*. 2nd ed. Hoboken, NY: John Wiley & Sons; 2006.
14. Bard AJ, Faulkner LR. Electrochemical methods: fundamentals and applications. *Rus J Electrochem*. 2002;38:1364-1365.
15. Iizuka M, Koyama T, Kondo N, Fujita R, Tanaka H. Actinides recovery from molten salt/liquid metal system by electrochemical methods. *J Nucl Mater*. 1997;247:183-190.
16. Kobayashie T, Fujita R, Nakamura H, Koyama T. Evaluation of cadmium pool potential in a electrorefiner with ceramic partition for spent metallic fuel. *J Nucl Sci Technol*. 1997;34:50-57.
17. Nawada HP, Bhat NP, Balasubramanian GR. Thermochemical modeling of electrorefining process for reprocessing spent metallic fuel. *J Nucl Sci Technol*. 1995;32:1127-1137.
18. Kuratal M, Yahagi N, Kitawaki S, Nakayoshi A, Fukushima M. Sequential electrolysis of U-Pu alloy containing a small amount of Am to recover U- and U-Pu-Am products. *J Nucl Sci Technol*. 2009;46:175-183.
19. Koyama T, Kinosmta K, Inoue T, et al. Study of molten salt electrorefining of U-Pu-Zr alloy fuel. *J Nucl Sci Technol*. 2002; 39:765-768.
20. Sohn S, Choi S, Park J, Hwang S. Computational model-based design of molten salt electrorefining process for high-purity zirconium metal recovery from spent nuclear fuel. *Int J Energy Res*. 2020. https://doi.org/10.1002/er.5724.
21. Fredrickson GL, Yoo T-S. Liquid cadmium cathode performance model based on the equilibrium behaviors of U and Pu in molten LiCl-KCl/Cd system at 500°C. *J Nucl Mater*. 2020; 528:151883.
22. Johnson I, Chasanov MG, Yonco RM. Pu-Cd system: thermodynamics and partial phase diagram. *Trans Metallurg Soc AIME*. 1965;233:1408-1414.
23. Roy J, Grantham L, Grimmett D, et al. Thermodynamic properties of U, Np, Pu, and Am in molten LiCl-KCl eutectic and liquid cadmium. *J Electrochem Soc*. 1996;143:2487-2492.
24. Koyama T, Iizuka M, Kondo N, Fujita R, Tanaka H. Electrodeposition of uranium in stirred liquid cadmium cathode. *J Nucl Mater*. 1997;247:227-231.
25. Masatoshi I, Koichi U, Tadashi I, Takashi I, Osamu S, Yasuo A. Development of plutonium recovery process by molten salt electrorefining with liquid cadmium cathode. *Proceedings of 6th International Exchange Meeting on Actinide and Fission Product Partitioning and Transmutation*. Madrid, Spain: Nuclear energy agency organisation for economic co-operation and development; 2000:327-341.
26. Sakamura Y, Murakami T, Tada K, Kitawaki S. Electrowinning of U-Pu onto inert solid cathode in LiCl-KCl eutectic melts containing UCl_3 and $PuCl_3$. *J Nucl Mater*. 2018;502:270-275.
27. Nishimura T, Koyama T, Iizuka M, Tanaka H. Development of an environmentally benign reprocessing technology-pyrometallurgical reprocessing technology. *Prog Nucl Energy*. 1998;32:381-387.
28. Laidler JJ, Battles JE, Miller WE, Ackerman JP, Carls EL. Development of pyroprocessing technology. *Prog Nucl Energy*. 1997;31:131-140.
29. Koyama T, Fujita R, Hzuka M, Sumida Y. Pyrometallurgical reprocessing of fast reactor metallic fuel—development of a new electrorefiner with a ceramic partition. *Nucl Technol*. 1995;110:357-368.
30. Raj B, Kamath HS, Natarajan R, Rao PRV. A perspective on fast reactor fuel cycle in India. *Prog Nucl Energy*. 2005;47:369-379.
31. Nagarajan K, Reddy BP, Ghosh S, et al. Development of pyrochemical reprocessing for spent metal fuels. *Energy Procedia*. 2011;7:431-436.
32. Martinot L. Some thermodynamic properties of dilute solutions of actinide chlorides in (Li-K)Cl and in (Na-K)Cl eutectics. *J Inorg Nucl Chem*. 1975;37:2525-2528.
33. Seo S, Choi S, Park BG. Transient modeling of spent nuclear fuel electrorefining with liquid metal electrode. *J Nucl Mater*. 2017;491:115-125.
34. Serp J, Konings RJM, Malmbeck R, Rebizant J, Scheppler C, Glatz J-P. Electrochemical behaviour of plutonium ion in LiCl-KCl eutectic melts. *J Electroanal Chem*. 2004;561:143-148.
35. Kobayashi T, Fujita R, Nakamura H, Koyama T, Iizuka M. Electrorefining experiments to recover uranium with a cadmium-lithium anode and their theoretical evaluation. *J Nucl Sci Technol*. 1999;36:288-296.
36. Merwin A, Phillips WC, Williamson MA, Willit J, Motsegood PN, Chidambaram D. Presence of Li clusters in molten LiCl-Li. *Sci Rep*. 2016;6:25435.
37. Gonzalez M, Hansen L, Rappleye D, Cumberland R, Simpson MF. Application of a one-dimensional transient electrorefiner model to predict partitioning of plutonium from curium in a pyrochemical spent fuel treatment process. *Nucl Technol*. 2015;192:165-171.
38. Cumberland RM, Yim MS. Development of a 1D transient electrorefiner model for pyroprocess simulation. *Ann Nucl Energy*. 2014;71:52-59.
39. Ahluwalia RK, Hua TQ, Geyer HK. Removal of zirconium in electrometallurgical treatment of experimental breeder reactor II spent fuel. *Nucl Technol*. 2001;133:103-118.
40. Ahluwalia RK, Geyer HK. Electrotransport of uranium from a liquid cadmium anode to a solid cathode. *Nucl Technol*. 2002; 140:41-50.
41. Ahluwalia RK, Hua TQ, Vaden DE. Uranium transport in a high-throughput electrorefiner for EBR-II blanket fuel. *Nucl Technol*. 2004;145:67-81.
42. Iizuka M, Kinoshita K, Koyama T. Modeling of anodic dissolution of U-Pu-Zr ternary alloy in the molten LiCl-KCl electrolyte. *J Phys Chem Solid*. 2005;66:427-432.
43. Lee JH, Kang YH, Hwang SC, Lee HS, Kim EH, Park SW. Assessment of a high-throughput electrorefining concept for a spent metallic nuclear fuel—I: computational fluid dynamics analysis. *Nucl Technol*. 2008;162:107-116.
44. Lee JH, Oh KH, Kang YH, et al. Assessment of a high-throughput electrorefining concept for a spent metallic nuclear fuel—II: electrohydrodynamic analysis and validation. *Nucl Technol*. 2009;165:370-379.
45. Kim KR, Bae JD, Park B-G, et al. Modeling and analysis of a molten-salt electrolytic process for nuclear waste treatment. *J Radioanal Nucl Chem*. 2009;280:401-404.

46. Kim KR, Choi SY, Kim JG, et al. Multi physics modeling of a molten-salt electrolytic process for nuclear waste treatment. *IOP Conf Ser Mater Sci Eng*. 2010;9:012002.
47. Iizuka M, Moriyama H. Analyses of anodic behaviour of metallic fast reactor fuel using a multidiffusion layer model. *J Nucl Sci Technol*. 2010;47:1140-1154.
48. Iizuka M, Omori T, Tsukada T. Behaviour of U-Zr alloy containing simulated fission products during anodic dissolution in molten chloride electrolyte. *J Nucl Sci Technol*. 2010;47:244-254.
49. Murakami T, Kato T, Rodrigues A, et al. Anodic dissolution of irradiated metallic fuels in LiCl-KCl melt. *J Nucl Mater*. 2014;452:517-525.
50. Venkatesh A, Ghosh S, Vandarkuzhali S, Prabhakara Reddy B, Nagarajan K, Vasudeva Rao PR. Modeling the anodic behavior of U, Zr, and U-Zr alloy in molten LiCl-KCl eutectic. *Nucl Technol*. 2013;182:98-110.
51. Ghosh S, Vandarkuzhali S, Gogoi N, et al. Anodic dissolution of U, Zr and U-Zr alloy and convolution voltammetry of $Zr^{4+}|Zr^{2+}$ couple in molten LiCl-KCl eutectic. *Electrochem Acta*. 2011;56(24):8204-8218.
52. Iizuka M, Akagi M, Omori T. Development of treatment process for anode residue from molten salt electrorefining of spent metallic fast reactor fuel. *Nucl Technol*. 2012;181:507-525.
53. Iizuka M, Inoue T, Shirai O, Iwai T, Arai Y. Application of normal pulse voltammetry to on-line monitoring of actinide concentrations in molten salt electrolyte. *J Nucl Mater*. 2001;297:43-51.
54. Nagai T, Uehara A, Fujii T, Shirai O, Yamana H. In-situ measurement of UO_2 concentration in molten $NaCl_2CsCl$ by differential pulse voltammetry. *J Nucl Sci Technol*. 2006;43:1511-1516.
55. Chang YI. The integral fast reactor. *Nucl Technol*. 1989;88:129-138.
56. Chang YI. Technical rationale for metal fuel in fast reactors. *Nucl Eng Technol*. 2007;39:161-170.
57. Keiser DD Jr, Mariani RD, Zr-rich layers electrodeposited onto stainless steel cladding during the electrorefining of EBR-II fuel. *J Nucl Mater*. 1999;270:279-289.
58. Mariani RD, Porter DL, O'Holleran TP, Hayes SL, Kennedy JR. Lanthanides in metallic nuclear fuels: their behavior and methods for their control. *J Nucl Mater*. 2011;419:263-271.
59. Shishkin VY, ed. *Development of the Physical and Chemical Basis of the Behavior of Uranium Oxides, REM and Anode Processes in Chloride Melts, Stage 2018, Report, State Registration Number* AAAA-A*18-118070690009-1, Inv. No. 226/2018*. Yekaterinburg, Russia: Institute of High Temperature Electrochemistry Ural Department of the Russian Academy of Sciences (IHTE UB RAS); 2018.
60. Kisza IA, Kazmierczak J. Kinetics of electrode reactions on metallic electrodes in pure molten chlorides. *Chem Papers*. 1991;45:187-194.
61. Despic R, Jovic V. Electrochemical deposition and dissolution of alloys and metal composites–fundamental aspects. *Mod Asp Electrochem*. 1995;27:143-232.
62. Kadota K, Shimosaka A, Shirakawa Y, Hidaka J. Dehydration process in NaCl solutions under various external electric fields. *J Nanopart Res*. 2007;9:377-387.
63. Serp J, Chamelot P, Fourcaudot S, et al. Electrochemical behaviour of americium ions in LiCl-KCl eutectic melt. *Electrochim Acta*. 2006;51:4024-4032.
64. Murakami T, Sakamura Y, Akiyama N, Kitawaki S, Nakayoshi A, Fukushima M. Anodic behaviour of a metallic U-Pu-Zr alloy during electrorefining process. *J Nucl Mater*. 2011;414:194-199.

How to cite this article: Galashev AY. Processing of fast neutron reactor fuel by electrorefining: Thematic overview. *Int J Energy Res*. 2020;1–20. https://doi.org/10.1002/er.6267